Effect of magnetized electron cooling on a Hopf bifurcation

S.Y. Lee,[1] M. Ball,[1] B. Brabson,[1] J. Budnick,[1] D.D. Caussyn,[1,*] P. Colestock,[2] G. East,[1] M. Ellison,[1] B. Hamilton,[1] K. Hedblom,[3] X. Kang,[1] D. Li,[1] J.Y. Liu,[1] K.Y. Ng,[3] A. Pei,[1] A. Riabko,[1] M. Syphers,[4] and L. Wang[1]

[1]*Indiana University Cyclotron Facility, 2401 Milo B. Sampson Lane, Bloomington, Indiana 47408*

[2]*Fermilab, P.O. Box 500, Batavia, Illinois 60510*

[3]*Uppsala University, The Svedberg Laboratory, Box 533, S-75121, Uppsala, Sweden*

[4]*Alternate Gradient Synchrotron, Brookhaven National Laboratory, Upton, New York 11973*

(Received 5 September 1995)

We have observed longitudinal limit cycle oscillations of a proton beam when a critical threshold in the relative velocity between the proton beam and the cooling electrons has been exceeded. The threshold for the bifurcation of a fixed point into a limit cycle, also known as a Hopf bifurcation, was found to be asymmetric with respect to the relative velocity. Further experiments were performed to verify that the asymmetry was related to electron beam alignment with respect to the stored proton beam. The measured amplitudes of the ensuing limit cycle were used to determine the cooling drag force, which exhibits the essential characteristics of the magnetized cooling, where the limit cycle attractor can coexist with a damping-free region and/or a fixed point attractor.

PACS number(s): 29.27.Bd, 41.75.−i, 03.20.+i, 05.45.+b

Since its invention by Budkar in 1966, *electron cooling* has been widely applied to many storage rings for atomic, nuclear, particle, and accelerator physics research [1,2]. In order to optimize machine operation and luminosity for physics experiments, beam dynamics studies with electron cooling have been of considerable interest in accelerator physics [3–7].

Recently, we have reported an experimental observation of the Hopf bifurcation in the synchrotron phase space when the relative velocity between the proton beam and the cooling electrons is greater than a threshold value [4,5]. We have found that the threshold of bifurcation is related to the "temperature" or equivalently the longitudinal rms velocity spread of cooling electrons seen by protons. In these experiments, we were puzzled by the asymmetry of the bifurcation with respect to the relative velocities (see Fig. 1 of Ref. [4] and Figs. 4 and 5 of Ref. [5]).

Because the asymmetric bifurcation can arise from the combination of nonzero dispersion functions and the space charge depression of cooling electrons, we investigate the effect of electron beam alignment on the threshold of Hopf bifurcation and the shape of the cooling drag force on the amplitude of limit cycle attractor. In this paper, we report results of experimental studies on Hopf bifurcation by varying the electron beam direction relative to the proton beam. Our experimental data are used to obtain the drag force which can reflect the effects of magnetized cooling. The dependence of stable particle motion on the shape of the cooling drag force has also been studied in extensive numerical simulations.

The IUCF Cooler Ring is a hexagonal shaped storage ring with a circumference of 86.8 m [2]. The experiment was done with a 45 MeV proton beam injected and then stored with a 10 s cycle time. After 5 s from the start of the cycle, the six dimensional phase space coordinates were digitized at ten-revolution intervals for 16 384 points [6,7]. The nominal rf cavity frequency was 1.031 68 MHz with the harmonic number $h = 1$. The beam was typically a single bunch of about 4×10^9 protons with a typical length of about 100 ns full width at half maximum (FWHM) with the rf peak voltage being about 41 V. For the experimental results reported in this paper, the rf voltages were set at 85 V and 128 V. Since measurements of longitudinal motion were being made, the phase lock feedback loop for the rf, which is normally on, was switched off.

The synchrotron motion is characterized by the phase ϕ, which is the phase of a particle relative to the rf cavity voltage, and its conjugate momentum variable $\delta = \frac{\Delta p}{p}$, which is the fractional momentum deviation of the particle from that of the synchronous particle. The difference equations describing the synchrotron motion are

$$\delta_{n+1} = \delta_n - \frac{2\pi\nu_s^2}{h\eta}(\sin\phi_n - \sin\phi_s) - f(\delta_n), \quad (1)$$

$$\phi_{n+1} = \phi_n + 2\pi h\eta\delta_{n+1}, \quad (2)$$

where $\eta = -0.86$ is the phase slip factor, ϕ_s is the phase of the synchronous particle, which for a stored beam is 0°, h is the harmonic number, $f(\delta)$ is the damping force resulting from electron cooling, and the subscripts n refer to the revolution number. The small amplitude synchrotron tune ν_s at the zero synchronous phase is related to the rf cavity voltage $V_{\rm rf}$ by $\nu_s = \sqrt{h|\eta|eV_{\rm rf}/2\pi E\beta^2}$, where e, βc, and E are, respectively, the charge, the speed, and the total energy of the proton. The angular synchrotron frequency is given by $\omega_s = \omega_0\nu_s$, where ω_0 is the angular revolution frequency.

The damping force $f(\delta)$ produced by the electron cooling is the result of a statistical exchange of energy in Coulombic collisions between the protons and relatively cold electrons as they travel together in the accelerator. In practice, electron cooling in synchrotrons is normally done in relatively short straight sections due to cost and space limitations. At IUCF the electron beam is mixed

*Present address: Department of Physics, Florida State University, Tallahassee, FL 32306.

with the proton beam for distance of only 2.2 m or about 2.5% of the accelerator circumference. The electron beam radius is about 1.27 cm and the cathode temperature is about 1300 K or $kT_{\rm cath} = 0.11$ eV, where k is the Boltzmann constant. The maximum electron beam current is 4 A. The electron beam current used in this experiment was 0.956 A.

Assuming an electron beam with an isotropic phase space Maxwellian velocity distribution, the damping force in the nonmagnetized binary collision theory is given by

$$f(\delta) = \frac{4\pi\alpha\Delta_{e\|}}{\omega_0} g(\zeta), \tag{3}$$

with a kinematic factor given by $g(\zeta) = g_0(\zeta)$ with

$$g_0(\zeta) = \frac{3\sqrt{\pi}}{4\zeta^2}\left[\mathrm{erf}(\zeta) - \frac{2\zeta}{\sqrt{\pi}} e^{-\zeta^2}\right], \tag{4}$$

where α is the $1/e$ damping rate for small relative velocities, $\Delta_{e\|} = \sigma_e/\beta c$ with σ_e as the rms velocity of cooling electrons, and $\zeta = (\delta - \delta_e)/\Delta_{e\|}$ with δ_e as the fractional momentum deviation of the proton traveling at the velocity of cooling electrons with respect to the synchronous particle of the rf cavity. From our previous measurements [4,5], we have $\alpha \approx 40\ \mathrm{s}^{-1}$ and $\Delta_{e\|} \approx 3 \times 10^{-4}$ for the IUCF electron cooling system for a proton kinetic energy of 45 MeV.

The effective temperature of the electron beam is related to the rms electron velocity spread by

$$kT_{\|\mathrm{eff}} = \frac{1}{2} m_e \sigma_e^2 = \frac{1}{2} m_e \beta^2 c^2 \Delta_{e\|}^2. \tag{5}$$

Because of the adiabatic acceleration, the longitudinal effective electron temperature is much smaller than that of the cathode temperature. Since there is no adiabatic damping in the transverse phase space, the effective transverse temperature remains 0.11 eV, which gives an equivalent momentum deviation of $\Delta_{e\perp} = 2.2 \times 10^{-3}$. For comparison, the bucket height of the synchrotron phase space at a rf voltage of 128 V is about 1.0×10^{-3}.

Since the cooling drag force of Eq. (4) is maximum at $|\delta - \delta_e| \approx \Delta_{e\|}$, it is evident that the center of the rf phase space will become unstable when $|\delta_e| > \Delta_{e\|}$ [4,5]. The stability is ensured only if the damping effect of synchrotron motion with $\delta > 0$ has exactly been cancelled by the excitation of synchrotron motion in the region $\delta < 0$, or vice versa. The cancellation of the damping and the excitation in the synchrotron motion leads to the limit cycle attractor.

Since the threshold of Hopf bifurcation is related to the rms velocity spread of cooling electrons along the proton trajectory, the asymmetric Hopf bifurcation can arise from different velocity spreads affecting protons having a different momentum closed orbit. The increase in the rms velocity spread can result from a misaligned proton beam in combination with the space charge depression of the electron beam [see Eq. (98) of Ref. [1]]. Thus the misalignment of the cooling electron beam can contribute to the asymmetry in the Hopf bifurcation, which was commonly observed in our earlier experiments. For a properly aligned electron beam, space charge depression will shift the relative velocity without affecting the velocity spread.

Since electrons having speed identical to that of protons have a much smaller momentum rigidity, the electron beam alignment can easily be achieved by superimposing a horizontal or a vertical dipole field to the solenoidal field. A method to obtain an "optimal" alignment is described as follows: When the rf frequency is shifted, the beam, which is originally at the center of the rf bucket (i.e., $\delta = 0$ and $\phi = 0$), will be dragged away from the origin and undergo synchrotron oscillations. If the damping force were linear over the entire range of relative velocity $v_{\rm rel}$, the proton beam would damp to a new fixed point attractor $\phi_{\rm FP}$, where

$$\phi_{\rm FP} \approx \frac{2\alpha}{\omega_0 \nu_s} \frac{h\eta\delta_e}{\nu_s}. \tag{6}$$

The resulting $\phi_{\rm FP}$ is the synchronous phase angle ϕ_s of the beam.

In order to permit us to precisely measure the synchronous phase angle $\phi_{\rm FP}$ shown in Eq. (6), we choose a small rf cavity voltage with $V_{\rm rf} = 10$ V, where the corresponding synchrotron tune is 1.25×10^{-4} at $h = 1$. The rf synchronous phase angle is measured by stepping away from the reference frequency by 200 Hz [8]. Figure 1 shows the drag force, which is $eV_{\rm rf} \sin\phi_{\rm FP}$, vs the horizontal and vertical dipole currents (in digital analog converter or DAC units), where the lower plot gives the drag force as a function of the vertical dipole strength $V_{\rm sol}$ with $H_{\rm sol} = 160$ DAC. The maximum drag force is found to be about 1.8 eV/turn. From Eq. (6), we obtain $\alpha = 45\ \mathrm{s}^{-1}$, which agrees well with the value of 40 s^{-1} obtained from an earlier measurement by using the harmonic modulation to the high voltage power supply (HVPS) (see Sec. III A of Ref. [5]).

To investigate the Hopf bifurcation due to the nonlinear damping force, the proton velocity was displaced from

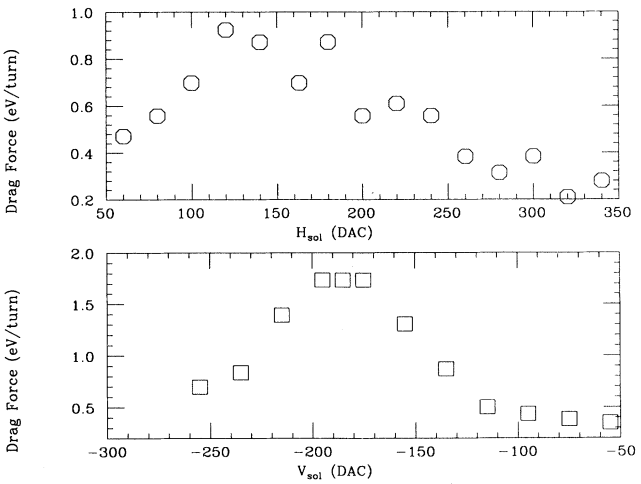

FIG. 1. The measured damping drag force is plotted vs the horizontal and the vertical electron beam alignments in the upper and lower plots, respectively. The lower plot shows the drag force vs $V_{\rm sol}$ with an optimal $H_{\rm sol} = 160$ DAC value obtained from the upper plot. The DAC (digital analog converter) unit in the coordinate is proportional to the current applied to the dipole coil winding.

the electron velocity by changing the rf cavity frequency, where a step of 1 Hz resulted in changing the fractional proton velocity by about 1×10^{-6}. Let f_0 be the rf cavity frequency when the synchronous proton travels at the same velocity as that of cooling electrons. At a new rf frequency f, the fractional momentum deviation δ_e of the electron beam from the proton beam becomes

$$\delta_e = \frac{(f - f_0)}{\eta f_0}. \tag{7}$$

The maximum synchrotron phase amplitude $\hat{\phi}$ and the maximum fractional momentum deviation $\hat{\delta}$ are measured at 5 s after the start of an injection cycle to allow the initial transient oscillations to damp out.

As shown in our earlier reports [4,5], the amplitudes of limit cycle attractors can also be measured by using an oscilloscope to measure the longitudinal profile from the beam position monitor (BPM) sum signal. The measured amplitudes with the optimal drag force at $H_{\rm sol} = 160$ DAC, $V_{\rm sol} = -185$ DAC, and $V_{\rm rf} = 128$ V are shown in Fig. 2(b). The corresponding beam intensity normalized to the peak current is shown in Fig. 2(a). Note in particular that Fig. 2 shows a nearly symmetric amplitude of limit cycle vs δ_e and a close correlation between the storage beam current and the Hopf bifurcation threshold [9]. On the other hand, when the electron and proton beams were not properly aligned, we always observed asymmetric Hopf bifurcations.

To understand the nature of this instability, the dashed line shown in Fig. 2(b) is the result of computer simulations using Eqs. (1) and (2) with a damping force of Eqs. (3) and (4) for $\Delta_{e\|} = 1.89 \times 10^{-4}$, or $kT_{\|} = 8 \times 10^{-4}$ eV. Thus the temperature of the properly aligned cooling electron beam appears to be colder than what has been observed earlier [4,5]. We note also that amplitudes of limit cycle attractors are smaller than those predicted by the drag force model of Eq. (4).

When the cooling electron beam is magnetically confined by a solenoidal field, such as the IUCF Cooler Ring, the damping force can be decomposed into two components, where the magnetized cooling can enhance the effective longitudinal and transverse cooling rates (see

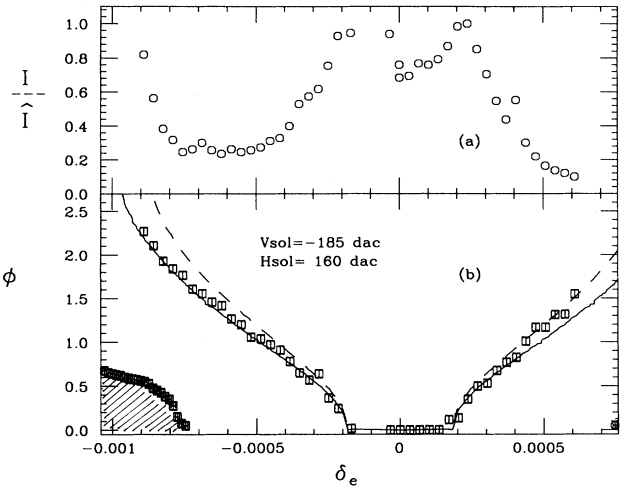

FIG. 2. The measured amplitude of limit cycle attractor and the storage beam current observed vs δ_e as defined in Eq. (7) for the optimized cooling alignment, which provides a nearly symmetric Hopf bifurcation. The dashed line is obtained from numerical simulations with kinematic factor (4) with $\Delta_{e\|} = 1.89 \times 10^{-4}$. The tracking was done for the time equivalent of $160\tau \approx 4$ s, where the damping time is $\tau = 1/\alpha$. The solid line is the limit cycle attractor and the shaded area in the lower left corner of the plot (b) is the region that converges to the fixed point attractor, obtained from numerical simulations using the kinematic factor (9) with $\Delta_{e\|} = 1.8 \times 10^{-4}, \Delta_{e\perp} = 2.2 \times 10^{-3}$, $A_{\|} = 1$, and $A_{\perp} = 0.5$.

Fig. 15 of Ref. [1]), and the longitudinal cooling force may exhibit two peaks. We are particularly interested in determining the cooling drag force for relative velocities lying between the longitudinal and transverse rms values. The measured amplitudes of limit cycle attractors enable us to study the drag force at the relative momentum deviation δ_e lying in the range of $(\Delta_{e\|}, \Delta_{e\perp})$.

In the presence of magnetized cooling, the cooling drag force can be divided into two components, where the adiabatic component is maximum at the rms longitudinal velocity spread of cooling electrons and the nonmagnetized component is peaked at the transverse rms velocity spread of cooling electrons. Thus we simulate the magnetized cooling with the following simplified drag force model represented by straight lines:

$$g(\zeta) = \begin{cases} \zeta & \text{if } 0 \le \zeta < \zeta_1 \\ \zeta_1 + S_1(\zeta - \zeta_1) & \text{if } \zeta_1 \le \zeta < \zeta_2 \\ \zeta_1 + S_1(\zeta_2 - \zeta_1) + S_2(\zeta - \zeta_2) & \text{if } \zeta_2 \le \zeta < \zeta_3 \\ \zeta_1 + S_1(\zeta_2 - \zeta_1) + S_2(\zeta_3 - \zeta_2) + S_3(\zeta - \zeta_3) & \text{if } \zeta_3 \le \zeta < \zeta_4 \\ [\zeta_1 + S_1(\zeta_2 - \zeta_1) + S_2(\zeta_3 - \zeta_2) + S_3(\zeta_4 - \zeta_3)]\zeta_4^2/\zeta^2 & \text{if } \zeta_4 \le \zeta, \end{cases} \tag{8}$$

with $g(-\zeta) = -g(\zeta)$, $\zeta = (\delta - \delta_e)/D$, and $D = 3 \times 10^{-4}$. Figure 3 shows the final equilibrium phase amplitudes of 40 particles, which are initially uniformly distributed along the $\delta \ge 0$ axis by solving Eqs. (1) and (2) with $\nu_s = 0.0003, \eta = -0.86$. The corresponding drag force model of Eq. (8) with parameters $\zeta_1 = 1, S_1 = -0.05$, $\zeta_2 = 2, S_2 = 0$, $\zeta_3 = 4, S_3 = 0.05$, and $\zeta_4 = 5$ is shown in the upper plot. The following observations can be drawn. (1) $S_1 \le 0$ in the region $\zeta \in [1, 2)$ produces a limit cycle attractor. (2) $S_2 = 0$ in the region $\zeta \in [2, 4]$ produces a center *damping-free* core for $\delta_e/D \in [2, 4]$, where the center core and the limit cycle attractor coexist. The limit cycle attractor becomes discontinuous at $\delta_e/D \approx 3$. (3) The positive drag force slope of $S_3 = 0.05$ in the region [4,5] revitalizes the fixed point attractor for $\delta_e/D \in [4, 5]$. (4) For $\delta_e/D > 5$, the synchrotron motion becomes unstable, which has resulted from a higher excitation rate of synchrotron oscillations at $\delta \le 0$ than the damping of

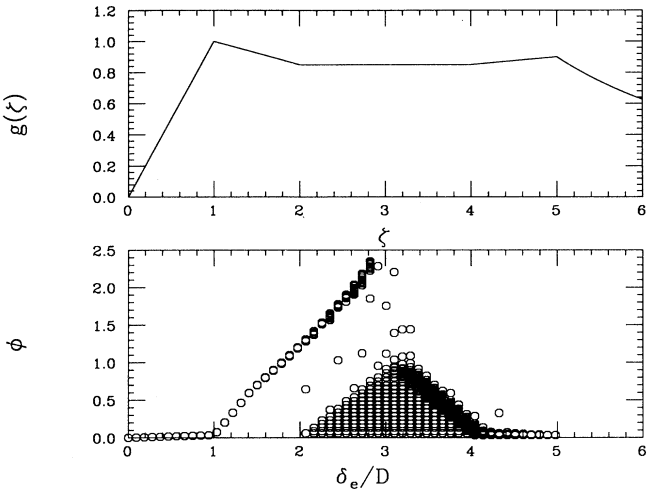

FIG. 3. The lower plot shows the attractor solution and the stable synchrotron amplitude obtained from numerical simulations vs δ_e/D. The upper plot shows the corresponding kinematic function of Eq. (8) with parameters $\zeta_1 = 1$, $S_1 = -0.05$, $\zeta_2 = 2$, $S_2 = 0$, $\zeta_3 = 4$, $s_3 = 0.05$, and $\zeta_4 = 5$ vs $\zeta = (\delta - \delta_e)/D$.

synchrotron motion at $\delta > 0$.

Motivated by the understanding attained from the above model, we postulate the kinematic function for the magnetized cooling as follows:

$$g(\zeta) = A_{\parallel} g_0(\zeta) + A_{\perp} g_0\left(\frac{\Delta_{e\parallel}}{\Delta_{e\perp}}\zeta\right), \qquad (9)$$

where $\zeta = (\delta - \delta_e)/\Delta_{e\parallel}$, $g_0(x)$ is given in Eq. (4), $\Delta_{e\parallel}$ and $\Delta_{e\perp}$ are, respectively, the longitudinal and transverse velocity spread of cooling electrons, and $A_{\parallel}$ and $A_{\perp}$ are, respectively, the adiabatic and the nonmagnetized drag force components. Such a cooling kinematic function can be obtained with the assumption of Maxwellian distribution functions for cooling electrons. The solid line in Fig. 2(b) is obtained from tracking calculation with parameters $\Delta_{e\parallel} = 1.8 \times 10^{-4}$, $\Delta_{e\perp} = 2.2 \times 10^{-3}$, $A_{\parallel} = 1, A_{\perp} = 0.5$, and the synchrotron tune $\nu_s = 4.46 \times 10^{-4}$. The shaded area in the lower left corner corresponds to initial phase amplitudes which damp to a fixed point attractor at the center of the phase space. A particle with an initial synchrotron amplitude outside the shaded area will damp to the limit cycle attractor or become unstable. Note in particular that a positive slope in the kinematic factor of Eq. (9) has simultaneously generated a limit cycle attractor and a fixed point attractor for $\delta_e \leq -0.000\,75$. The magnetized cooling at the relative velocity lying between the longitudinal velocity and the transverse velocity spreads created simultaneously a limit cycle attractor and a fixed point attractor at the center of the rf bucket. The existence of a fixed point attractor evidently provides the mechanism for a beam accumulation, which produced the higher proton beam current shown in Fig. 2 at $\delta_e < -0.0008$. Thus the electron cooling system is employing transverse velocity spread to enhance the synchrotron phase space damping when the relative velocity is larger than the longitudinal velocity spread of cooling electrons. Because of the aperture limitation of a realistic machine, such as the IUCF cooler ring, experimental measurements at $\delta_e > 0.0008$ were not possible.

From our experimental data and extensive numerical simulations, we summarize our findings as follows. The Hopf bifurcation occurs when the slope $S_1 \leq 0$. The center damping-free region can be created by a local zero slope in the damping force, i.e., Hopf bifurcation does not necessarily imply an unstable center fixed point. Furthermore, the limit cycle attractor can coexist with a fixed point attractor [see Fig. 2(b)].

In conclusion, we have studied the effect of electron beam alignment on the Hopf bifurcation. When the electron and proton beams were carefully aligned, the amplitudes of limit cycle attractors became symmetric with respect to the relative velocity between the cooling electrons and the synchronous proton. The nonmagnetized drag force model with the kinematic factor of Eq. (4) fails to fit the data when the amplitude of the limit cycle attractor is large. These data have been employed to determine the drag force in the region $(\Delta_{e\parallel}, \Delta_{e\perp})$, which shows some of the essential characteristics of the magnetized cooling, where a limit cycle and fixed point attractors can coexist. The transverse velocity spread of cooling electrons plays a key role in beam accumulation when $\delta_e \in (\Delta_{e\parallel}, \Delta_{e\perp})$. Extensive numerical simulations have been performed to study effects of the drag force on particle motion. We find that the limit cycle attractor can coexist with a stable center core if the slope of the damping force becomes zero. A possible application of this type of damping force is to create a more uniformly distributed beam bunch in order to reduce space charge force in a beam at low energies.

This work was supported by NSF Grant No. PHY-9221402 and DOE Grant No. DE-FG02-93ER40801.

[1] H. Poth, Phys. Rep. **196**, 135 (1990).
[2] R.E. Pollock, Annu. Rev. Nucl. Sci. **41**, 357 (1991).
[3] G.I. Budkar *et al.*, Part. Accel. **7**, 197 (1976).
[4] D.D. Caussyn *et al.*, Phys. Rev. Lett. **73**, 2857 (1994).
[5] D.D. Caussyn *et al.*, Phys. Rev. E **51**, 4947 (1995).
[6] S.Y. Lee *et al.*, Phys. Rev. Lett. **67**, 3768 (1991); D.D. Caussyn *et al.*, Phys. Rev. A **46**, 7942 (1992); J.Y. Liu *et al.*, Phys. Rev. E **49**, 2347 (1994); M. Ellison *et al.*, *ibid.* **50**, 4051 (1994).
[7] M. Ellison *et al.*, Phys. Rev. Lett. **70**, 591 (1993); H. Huang *et al.*, Phys. Rev. E **48**, 4678 (1993); D. Li *et al.*, *ibid.* **48**, R1638 (1993); M. Syphers *et al.*, Phys. Rev. Lett. **71**, 719 (1993); Y. Wang *et al.*, Phys. Rev. E **49**, 1610 (1994).
[8] The shift in frequency should be minimized to avoid the nonlinear region of the damping force. In our case, we measured the phase differences between ±100 Hz shifts in the revolution frequency f_0.
[9] The optimal cooling electron beam alignment depends on the closed orbit of the proton beam. Thus the optimal setting of $H_{\rm sol}$ and $V_{\rm sol}$ DAC values can be different for each run. In our experiment, we found that symmetric Hopf bifurcation occurred only when the electron beam was aligned with that of the proton beam. Thus asymmetric Hopf bifurcation can be used as a signature for the misaligned cooling electron beam.